

Received 5 December 2022, accepted 13 December 2022, date of publication 19 December 2022,
date of current version 22 December 2022.

Digital Object Identifier 10.1109/ACCESS.2022.3230591

RESEARCH ARTICLE

ROI-Fuzzy Based Medical Data Authentication Scheme for Smart Healthcare System

KAMRED UDHAM SINGH^{1,2}, LALAN KUMAR¹, (Graduate Student Member, IEEE),
SURBHI BHATIA³, ANKIT KUMAR⁴, ALHANOF KHALID ALMUTAIRI³,
AND MOHD ASIF SHAH^{5,6}

¹School of Computing, Graphic Era Hill University, Dehradun 248002, India

²Department of Computer Science and Information Engineering, National Cheng Kung University, Tainan 701, Taiwan

³Department of Information Systems, College of Computer Science and Information Technology, King Faisal University, Hofuf, Al hasa 36362, Saudi Arabia

⁴Department of Computer Engineering and Applications, GLA University, Mathura 281406, India

⁵Department of Economics, Kebri Dehar University, Kebri Dehar, Somali 3060, Ethiopia

⁶School of Business, Woxsen University, Hyderabad, Telangana 502345, India

Corresponding author: Mohd Asif Shah (drmohtdasifshah@kdu.edu.et)

ABSTRACT During the current pandemic, telemedicine applications encourage radiologists to consult patients remotely. Medical images are typically sent over the internet for easy access when diagnosing a patient. Intruders can manipulate these images during communication. Therefore, we require a method of authentication for these images that is capable of authenticating these images before diagnosis. To address these issues, a watermarking scheme has been developed within the scope of this paper. The foundation of anticipated watermarking system is Regions of Interest (ROI), using FRT to RONI, and converted into blocks; afterward, Hessenberg decomposition is applied on blocks selected by means of fuzzy logic. The binary watermark is quantized into the medical image. It has made the watermarking system non-fragile and secure. The proposed scheme's performance is evaluated on various attack situations, including noise and scale assaults. Watermarked pictures with enhanced PSNR ranging from 56.9902 to 57.2356 have been produced using the proposed technique. In particular, we achieved high NC values of 0.9801 on applying image processing attacks. A series of tests are performed on the system to determine its sensitivity, and the results are compared to protocols. The simulation results demonstrate that the suggested solution offers a high level of security while being imperceptible and robust to various attacks.

INDEX TERMS FRT, ROI, fuzzy, Hessenberg, watermarking.

I. INTRODUCTION

With the advent of the internet, digital-multi-media (DM) may be rapidly disseminated around the globe. Media files are being freely duplicated, shared, and disseminated. This benefit can sometimes lead to accidental violations of copyright law, which is why copyright protection is essential. Digital watermarking (DW) is a method of copyright protection [1]. When using this method (DW), information (a watermark) is permanently included in a multimedia file. If you need evidence that a DM belongs to you, a digital watermark might assist. Information may be retrieved from multimedia that has

been watermarked when necessary [2], [3]. Copyright protection using DWs is becoming increasingly commonplace in the telemedicine industry.

X-ray, MRI, CT-scan, and ultrasound images are all examples of diagnostic procedures that routinely make use of digital imaging technology. De-noising [4], segmenting [5], and compressing [6] medical images such that textures [7] may be extracted. Therefore, these medical images are widely disseminated [8], [9], [10] both within the hospital intranet and online. All of the medical images are stored in the hospital's database using DICOM criteria [11], [12]. There is a risk of intentional or unintentional manipulation due to the widespread dissemination of medical photographs. Consequences in terms of life-threatening diagnoses might be

The associate editor coordinating the review of this manuscript and approving it for publication was Ali Kashif Bashir¹.

quite serious. Therefore, it is crucial to strongly stress integrity and authenticity while conveying medical photographs both inside and outside of the institution. [13], [14]. In order to assert the validity of medical images, digital watermarking is a better solution. Usually, medical photographs contain image metadata and patient facts relating to the patient's medical report [15]. DICOM standard indicates that the image header comprises the generic metadata structure [16]. The metadata describes the patient information, medical imaging, and acquisition attributes. This information is vulnerable to being lost or manipulated, making the resultant image suspect. DW is a well-known strategy for handling the problem of unintended changes to medical images. In literature, integrity, authenticity, imperceptibility, and reversibility garnered little attention which are the key characteristics of any watermarking method [11], [13].

In conventional watermarking, the watermarks are permanently entrenched into the whole of the cover image by modifying certain data. It is possible to separate a medical image into a diagnostic region of interest (RIO) and a non-diagnostic background region of interest (RONI) [17], [18]. It is possible to employ the RIO to permanently embed the watermark that causes pixel distortion and, ultimately, the incorrect diagnosis, in medical photos. Since this area is of little diagnostic value, RONI is employed to firmly plant the watermark there. Since the perceptual quality might modify the visual effect of medical diagnosis digital images, they are rigorously limited to prevent any distortion. In addition to posing a direct hazard to the patient's life, the risk of a misdiagnosis increases when such data is tampered with [13]. Numerous frequency-domain watermarking techniques have been developed to ensure reliability. Multiresolution representation, frequency localisation, and multi-scale analysis are all available in the frequency-domain, making it a useful tool for JPEG image standards [19], [20], [21]. However, RIO and RONI are components of digital medical images. Researchers have claimed that the region of interest (RONI) in a medical image should be carefully chosen so that a watermark may be embedded safely there since it comprises non-essential information and conveys the least amount of information. Utilizing the spatial domain RIO, a new method of image authentication has been presented [22]. Multiple watermarking techniques have been presented in [23] for tamper detection in medical photographs as a means of regulating patient privacy. Modulo operation on the block is used in another suggested effort for tamper detection and recovery [24], [25].

The above study motivated us to propose, a blind watermarking approach based on image segmentation. The technique targets medical imaging with a specific area that requires extra focus. To increase the security of medical images, the technique makes use of certain characteristics inside the images themselves. The medical image is separated into two separate areas called RIO and RONI. Further, the color channels of the RONI area have been separated as RGB. The green channel of RONI is transformed using FRT to obtain the coefficients and converted into blocks of

size 4 by 4. In order to entrench the watermark into these blocks, the blocks are selected using fuzzy logic. Further, the selected blocks are decomposed by Hessenberg decomposition, and finally the watermark is quantized into the Q matrix.

This paper follows the structure described below. Section 2 provides context for our work by providing an overview of several watermarking systems or strategies. The proposed research plan for the watermarking embedding and recovery procedure is outlined in Section 3. In Section 4, we will discuss a method for watermarking, and in Section 5, we will discuss the results of implementing this method. The final broad conclusion is presented in Section 5.

II. BACKGROUND AND RELATED WORK

Several methods of watermarking medical images have been published. When it comes to watermarking, many professionals like using the frequency domain. For JPEG picture standards, the frequency domain enables multiresolution representation, frequency localization, and multi-scale analysis [19], [20]. However, both RIO and RONI can be found in digitised medical imaging. Many studies concluded that the region of interest (RONI) should be appropriately selected in a medical image since it contains non-essential information and gives the least information, making it a good candidate for embedding a watermark [21].

The use of chaotic systems and return on investment (ROI) in watermarking has been increasingly common in recent years due to their proven reliability. It is possible to implement the segmentation method to separate medical images into regions of interest and regions of non-interest. Medical photos include essential information; consequently, watermarking technology should be carefully applied to ensure quality. Utilizing the spatial domain RIO, a new method of image authentication has been presented [22]. Multiple watermarking techniques have been presented in [23] for alteration detection in medical photographs as a means of regulating patient privacy. Modulo operation on the block is used in another suggested effort for tamper detection and recovery [24], [26]. To further authentication & safety of medical photographs, a watermarking technique was devised that makes use of a differential expansion approach based on neighbouring pixel values [27], [28], [29]. A bipolar multiple base conversion approach to disguise various encrypted data into a single image has been suggested in [30]. Watermarking has been proposed in [31] and [32] as a means of concealing sensitive patient data.

For watermark entrenchment in RONI, [33] proposes a method that segments the image into blocks and usages the LSB replacement method. An entrenching system for hybrid watermarks that combines encryption with watermarking [34]. The dual watermarking approaches presented in [35] and [36] are a system to identify manipulation and retrieve information from medical photographs. Using SHA-256, a blind and vulnerable reversible watermark entrenching system has been devised. It recalculates the hash data [27] to verify the health of the image file.

Similar methods are given in [37] for checking whether or not a ROI is genuine, finding any tampered blocks inside it, and restoring the original. Watermarking the medical image involves computing a hash code with SHA-256 and concealing it in the image's boundaries using the region of interest.

In [38], a method of watermarking that may be undone is presented. This approach uses the ROI's feature-bit matrix for contrast enhancement and tamper detection, guaranteeing the ROI's reversibility. In [39], a new approach to medical picture authentication, they combined discrete wavelet transform and particle swarm optimization. Watermarked images with minimal distortion are generated using the proposed method of determining appropriate wavelet coefficients followed by using PSO to hide the watermark information. A high-payload, reversible watermarking approach for protecting medical photographs is presented in [40]. With this method, the grayscale values are broadened to increase the ROI's visibility. In [38], a robust watermark technique for digital radiography images that distinguishes between the backdrop and anatomical features. Histogram Shifting (HS) modulation is utilized in this approach to insidiously intrench a watermark.

III. PROPOSED SCHEME

Cover medical images may be separated into ROI and RONI using the watermarking method given here. This work is an extension of our previous work [41]. After that is done, RONI's colour channels may be broken down further into RGB. To permanently embed the binary watermark, we employ the green channel of the ROI. The coefficients of the FRT applied to ROI's green channel are translated into 4×4 blocks. Fuzzy logic is applied to the process of selecting blocks, as detailed in the following subsection III-A. Following a Hessenberg decomposition of the selected blocks, the binary watermark picture is quantized into the Q matrix. For the last step, a watermarked image is generated using inverse Hessenberg decomposition and inverse fast Fourier transform.

A. FUZZY BASED BLOCK SELECTION

When it comes to image segmentation for applications like remote sensing and medical imaging, the most popular and promising approach is a fuzzy C-Means clustering. We employ a hybrid approach that relies on the membership value function of nearby pixels to accomplish our goals. A generic membership function is represented by Equation 1. The initial representation of the membership function is f_{ij} . The pixels of the blocks are represented by $B_{(pk)}$. Incorporating the general membership function with membership function results in a function as shown in equation 2.

$$\xi_{ik}^u = \sum_{j \in B(pk)} f_{ij} \quad (1)$$

The pixels of cover medical image is partitioned into c clusters by calculating the membership function f_{ik}^u and

incorporating it into general membership function ξ_{ik}^u .

$$f_{ik}^u = \frac{f_{ik}^u \xi_{ik}^u}{\sum_{j=1}^c f_{ik}^u \xi_{ik}^u} \quad (2)$$

The pixels of cover medical image is partitioned into c clusters by calculating the membership function f_{ik}^u and incorporating it into general membership function ξ_{ik}^u .

B. FINITE RIDGELET TRANSFORM

To compute a finite ridgelet transform (FRIT), one must first apply a wavelet transform, and then a discrete radon transform calculation. Two phases calculate the finite radon transform (FRAT): In the radon projection, the 32 radial dimensions of an image are processed using an inverse fast Fourier transform (IFFT) in one dimension and a fast Fourier transform (FFT) in the other. A one-dimensional wavelet is applied in the three layers of putrefaction, confined to radial directions briefly through origin. To implement FRAT, we first map the photograph space to the projection space using a set of projections that account for the diverse perspectives from which the images were captured. The computation is important to process the as well as computer vision and pattern recognition & reconstruction of DICOM images a finite grid is constructed on FRAT real function. The radon projection is determined by designating the set points to build up a line on the lattice. For every pixel in the row, the original image's pixel could be transmitted and the histogram. At last, histogram information is segmented to enable mean values to be calculated. After employing the wavelet and radon transforms, the ridgelet transform becomes obvious, as explained by Alzu'bi in [42]. Each and every radon projection's output is wavelet transformed before being multiplied.

C. LOGISTIC MAPPING

The representation of complex equations in polynomial form of chaotic behaviour of non-linear mathematical equation is called logistic map [23], [43], as represented in equation. 3.

$$X_{n+1} = \mu \cdot x_n(1 - x_n) \quad (3)$$

where $x_n \in [0, 1]$ corresponds to the proportion of the standing population to the maximal possible population. The interval $[0, 4]$ is utilised as the value for the logistic map attribute value, which falls between 3.57 and 4. Moreover, the two-dimensional logistic map also allows for the study of the development of complicated phenomena such as basins and attractors. The actions of a two-dimensional logistic map are more intricate than those of a standard logistic map. Discrete two-dimensional logistic maps are defined mathematically by the equation 4, where r is the scheme parameter and (x_i, y_i) is the pair-wise point at the i^{th} iteration [43].

$$2D \text{ Logistic map } \begin{cases} x_{i+1} = r(3y_i + 1)x_i(1 - x_i) \\ y_{i+1} = r(3x_{i+1} + 1)y_i(1 - y_i) \end{cases} \quad (4)$$

D. HESSENBERG DECOMPOSITION

The factorisation of a nonspecific matrix M into the form of Hessenberg putrefaction is the factorisation of a nonspecific matrix M into the form of orthogonal similarity transformations [44] as shown in equation 5.

$$M = QHQ^T \tag{5}$$

when $i > j + 1, h_{ij} = 0$ since Q is an orthogonal matrix, and H is an upper Hessenberg matrix, so they cancel each other out. Commonly, Hessenberg putrefaction is accomplished by employing a householder matrix. It is possible to classify the Householder matrix (P) as an orthogonal matrix.

$$P = \frac{I_n - 2uu^T}{u^T u} \tag{6}$$

where u in R_n is a vector of non-zero and I_n is an identity matrix of size $n \times n$. When $n \times n$ is the size of A , the total process has $n - 2$ steps. As a result, the following is how Hessenberg decomposition is calculated:

$$\begin{aligned} H &= (P_1, P_2, \dots, P_{(n-3)}, P_{(n-2)})^T \\ &\quad A(P_1, P_2, \dots, P_{(n-3)}, P_{(n-2)}) \\ H &= Q^T A Q \\ A &= Q H Q^T \end{aligned} \tag{7}$$

In the proposed watermarking approach, both the FRT transform and the Hessenberg putrefaction are utilized. The proposed watermarking approach is imperceptible to human sight and extremely robust to a broad range of attacks. The FRT transform twice the original image size, increasing payload capacity. The watermark can be embedded in the host image twice as large. According to section III-D, the Hessenberg putrefaction converts a generic matrix M into orthogonal similarity transformations. Every colour channel is represented by a greyscale value between 0 and 255. The orthogonal matrix has minimal changes if and only if the pixel block is putrefactive by Hessenberg putrefaction. When looking at a unitary matrix, you'll notice that the components in the next column are quite similar to those of the previous column. To put it another way, no two components in Q are exactly same. Changing the next column slightly can increase the watermark's invisibility and durability. To achieve both strong watermarking and a large payload approach, the suggested method combines the usage of FRT with Hessenberg putrefaction. The watermark must be embedded in such a way that it can be retrieved from the image despite the existence of potential assaults on the image processing pipeline. As a result, frequency-domain transformations are widely employed in image watermarking. Subsection 3E describes the process of watermark embedding, while subsection 3F describes the extraction procedure.

E. WATERMARK EMBEDDING PROCESS

The process of entrenching a watermark is described here. Figure 1 shows a schematic of the proposed watermark entrench system. In step one, the cover medical image is

modified using FRT transform to produce coefficients. In step two, the collected data is used to make 4×4 blocks, which are then shuffled using a secret key. The shuffling of blocks guarantees the resilience of the watermarking scheme. In step three, we use the fuzzy logic equation stated in Eq. 2 to choose which blocks to use. The watermark bits are then inserted in an orthogonal matrix Q by performing a Hessenberg putrefaction on each of the chosen blocks. Since the elements of columns two of the orthogonal matrix are similar to those of the Q matrix, the watermark bits may be included there. The watermark bits are entrenched using the equation stated in equation 8. In step four, the watermark image gets jumbled up by use of a logistic map. In step five, the blocks are rearranged and inverse Hessenberg putrefaction is applied. In step six, an inverse Fast Fourier Transform is used to produce the watermarked image.

$$Q' = \begin{cases} \text{if } w \text{ is } 1 = Q_{2i} \cdot \alpha + T \\ \text{if } w \text{ is } 0 = Q_{2i} \cdot \alpha \end{cases} \tag{8}$$

Algorithm 1

- Input:** Host medical image and a watermark image
Output: watermarked image
Step 1: Let the cover medical image (H) and a watermark image (W).
Step 2: Transform H using FRT to get its coefficients. Apply logistic chaotic map to W .
Step 3: Convert the coefficients into non-overlapping blocks of 4×4 and shuffle randomly.
Step 4: Use Fuzzy logic to select the block and apply Hessenberg putrefaction on each block to get Q matrix.
Step 5: The watermark bits are quantized into Q matrix using equation 8.
Step 6: Apply inverse Hessenberg decomposition and re-shuffle the blocks.
Step 7: Apply Inverse FRT to obtain the watermarked image.

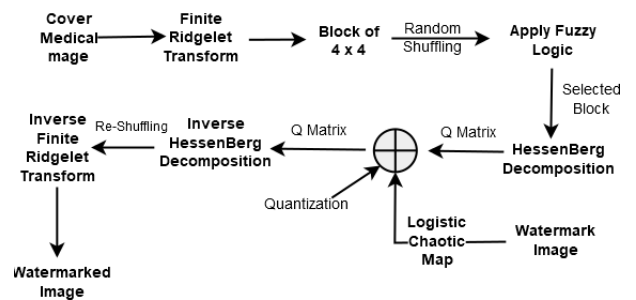


FIGURE 1. Watermark embedding process.

F. WATERMARK EXTRACTION PROCESS

In order to recover the watermark, firstly FRT is applied on the watermarked image. Secondly, the coefficients obtained

Algorithm 1

- Input:** Watermarked medical image
- Output:** Extracted watermark image
- Step 1:** Let the watermarked medical image (H').
- Step 2:** Transform H' using FRT to get its coefficients.
- Step 3:** Convert the coefficients into non-overlapping blocks of 4×4 and shuffle randomly.
- Step 4:** Use Fuzzy logic to select the block and apply Hessenberg putrefaction on each block to get Q matrix.
- Step 5:** The watermark bits are dequantized using equation 9.
- Step 6:** Extracted watermark

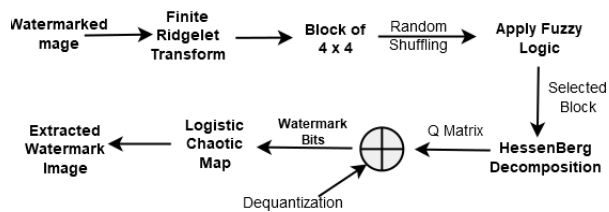


FIGURE 2. Watermark extraction process.

in previous step are used to create the blocks of 4×4 & randomly shuffled. Thirdly, Fuzzy logic is applied on each of the block to select and then selected blocks are decomposed using Hessenberg putrefaction and Q matrix is obtained. Forthly, the watermark bits are obtained using equation 9.

$$W(i) = \begin{cases} 1, & \text{if } \Delta \cdot Q'_{2i} > T \\ 0, & \text{otherwise} \end{cases} \quad (9)$$

IV. RESULTS AND DISCUSSION

The anticipated work has been examined in this section, and the results have been discussed. The effectiveness of the approach has been assessed using several color ultrasound picture types and binary watermark images. The chosen cover medical picture’s dimensions in the expected arrangement are 1024×768 pixels and 64×64 pixels for the watermark image. Figure 3 illustrates the test medical images and the watermark image. The cover image is segmented as ROI and RONI. The size of blocks used for watermark entrenching is 4×4 pixels. The proposed scheme is inspired by [45]. For watermark entrenching, the threshold value $T = 5$ has opted, and the value of $\Delta = 0.03$ is set. The of α is set to 0.05. This section also discusses the effects of different quality measures and results obtained during our experiment. Table 1 shows PSNR, NC, NPCR, and UACI of ultrasound medical images after watermarking process.

Six separate ultrasound images yielded PSNR values between 56 and 57 dB throughout the experiment. Our experimental PSNR values imply that our approach effectively hides watermarks from human eyes. Having a high PSNR indicates a low gain factor. Our experimental results demonstrates that the suggested system has a eminent factor and good imperceptibility of the watermarked image,

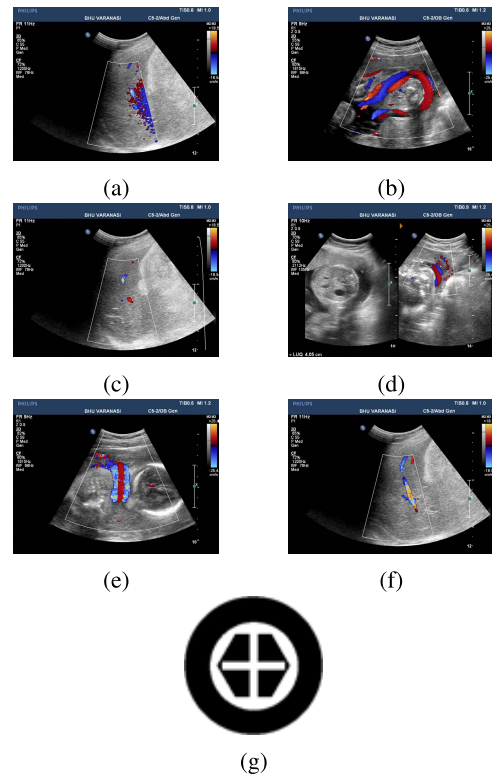


FIGURE 3. Ultrasound and watermark used in experiment.

as measured by NC values ranging from 0.97 to 0.98, which are summarised in Table 1. When viewing watermarked photos, the PSNR is more than 51 dB, and the NC value might go as high as 1. (i.e. 1.0). NPCR values calculated between the original and distorted watermarked photos signify a range of 0.81 to 0.98. Changes in pixel values as a function of time during the entrenching process. During the entrenching process, dramatic shifts may be seen in the UACI of watermarked photos. Here, the strength of the shifts is rather minor. The typical range for UACI is 0.30 to 0.32. In addition, when measuring the performance in terms of visual and perceptual quality, the total quality criteria indicate improvements. In this way, we may state that the expected technique works better when embedding bitmap watermark images into host colour ultrasound images.

TABLE 1. Performance of our scheme.

Image Name	PSNR	NC	NPCR	UACI
a	57.2356	0.9763	0.8909	0.3010
b	56.9863	0.9756	0.9299	0.3020
c	57.0123	0.9789	0.9032	0.3112
d	57.0311	0.9801	0.8901	0.3099
e	56.9902	0.9750	0.9233	0.3123
f	56.9696	0.9801	0.9301	0.3201

A. EVALUATION MATRICES

The quality of the original cover image becomes degraded when a watermark is entrenched into it or any alteration

TABLE 2. Multiple attacks against JPEG compression using varying quality parameters (QF).

QF	NC	SSIM
90	0.8423	0.8012
80	0.8615	0.8412
70	0.8656	0.8554
60	0.9696	0.8863
50	0.9756	0.8996
40	0.9901	0.9263

is made. As a result, it is essential to understand the cover image’s caliber [46]. The equation for calculating the peak signal-to-noise ratio (PSNR) is given in equation 10, and it can be used to quantify the level of likeness between the original image and the one that has been watermarked. dB is the unit that is used to measure the PSNR. The greater PSNR demonstrates that the original image and the one with the watermark are more comparable to one another.

$$PSNR = 10 \times \log_{10} \left(\frac{255^2}{MSE} \right) \quad (10)$$

Moreover, the error can also be measured through the mean squared error (MSE) between the original and watermarked image. Where C is the unaltered original image and CW is the altered watermarked version, the MSE may be calculated using the equation refMSE.

$$MSE = \frac{1}{M \times N} \sum_{x=0}^{M-1} \sum_{y=0}^{N-1} (C(x, y) - CW(x, y))^2 \quad (11)$$

Evaluating the quality of the retrieved watermark is an integral aspect of evaluating the effectiveness of the watermarking system. It is common practise for academics to take into account both the normalised correlation (NC) and the structural similarity index measure (SSIM) when assessing the robustness of a watermarking system [47]. The degree of similarity between the original and watermarked copies is evaluated by NC while SSIM analyses the structural similarities between the two images. Equations 12 and 13 can be used to determine the NC and the SSIM, respectively.

$$NC = \frac{\sum_{x=1}^M \sum_{y=1}^N w(x,y) \times w'(x, y)}{\sum_{x=1}^M \sum_{y=1}^N w^2(x, y)} \quad (12)$$

The recovered watermark image is denoted by iw' , whereas the original watermarked picture is denoted by w .

$$SSIM = \frac{(2\mu_w\mu_{w'} + C_1)(2\sigma_{ww'} + C_2)}{(\mu_w^2 + \mu_{w'}^2 + C_1)(\sigma_w^2 + \sigma_{w'}^2 + C_1)} \quad (13)$$

where μ_w corresponds to the mean of the original watermark and $\mu_{w'}$ corresponds to the mean of the recovered watermark, whereas σ_w and $\sigma_{w'}$ are the covariance of the original and extracted watermark, respectively, and C_1, C_2 are constants. The imperceptibility and resilience of the proposed watermarking procedure were put to the test using a variety of medical ultrasound images.

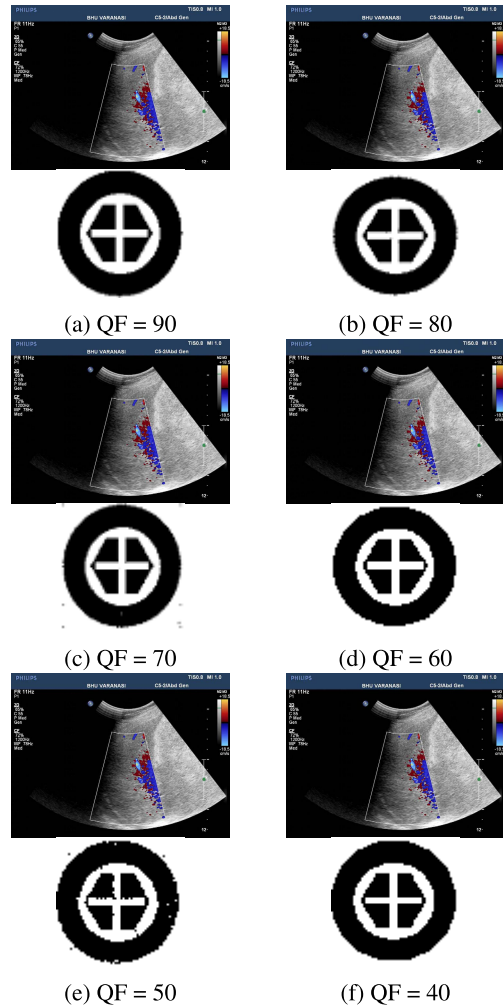


FIGURE 4. Watermarked Image and Extracted watermark after JPEG compression attacks with different quality factors.

B. ROBUSTNESS TEST

The watermarking scheme has been evaluated under various image processing attacks such as geometric and non-geometric. These image processing attacks (i.e., filtering, compression, noise, etc.) are interpolated on the watermarked image; afterward, the watermark is recovered. The robustness test of watermarking scheme is evaluated by calculating the NC and SSIM values of the recovered watermark. In this section and subsections, the results obtained after various image processing attacks have been discussed.

1) JPEG COMPRESSION ATTACK

During the pandemic, the diagnosis of the patients was made remotely. Therefore, communication channels frequently transfer medical images from one source to another. In this process, the medical images were compressed and converted from one format to another, either intentionally or unintentionally. Converting medical images from one format to another degrades the quality of the original image. Therefore, JPEG compression has become a very common and essential

TABLE 3. Watermarked image and extracted watermark after filtering attacks with different types with different filter masks.

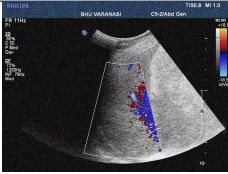

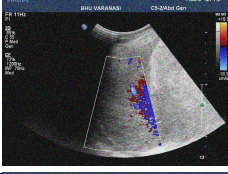

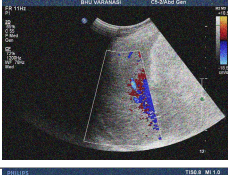

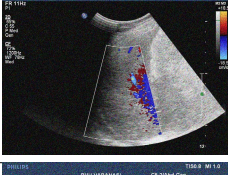

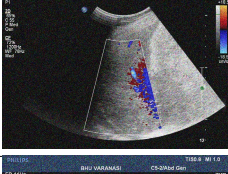

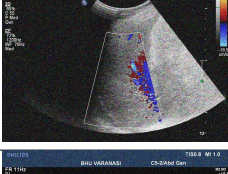

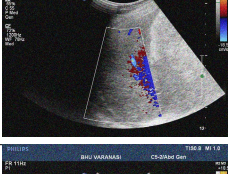

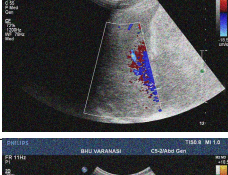

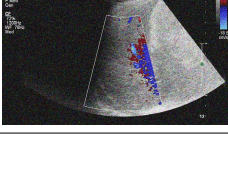

Attack Name	Filter Mask	Watermarked Image	Extracted Watermark
Median	3 x 3		
	5 x 5		
	7 x 7		
Average	3 x 3		
	5 x 5		
	7 x 7		
Low pass	3 x 3		
	5 x 5		
	7 x 7		

image processing attack. In figure 4, we can see corrupted and extracted watermarked images with different quality factors. Table 2 demonstrates the NC and SSIM values obtained in our experiment. The outcomes show that the expected method performed better than expected when subjected to a JPEG compression attack.

2) FILTERING ATTACK

The medical images are being compressed or converted either intentionally or unintentionally whenever transmitted over the communication channels. The signals in the communication channels distort the image. This distortion or signal processing attack is also interpolated on the watermark image. It is another kind of image processing attack known as a filter attack. In our experiment, we have also performed a filtering attack to assess the performance of the anticipated watermarking scheme. Table 3 represents a degraded watermarked image by filtering attack and the extracted watermark image with a different filter mask. Table 3 demonstrates the NC and SSIM values obtained in our experiment. The results demonstrate that the anticipated scheme outperformed under the JPEG compression attack.

TABLE 4. Filtering attacks with different types filter masks.

Attack Name	Filter Mask	NC	SSIM
Median	3 x 3	0.9511	0.9798
	5 x 5	0.8013	0.9615
	7 x 7	0.7801	0.8911
Average	3 x 3	0.8876	0.8703
	5 x 5	0.7413	0.8932
	7 x 7	0.7231	0.8933
Low pass	3 x 3	0.8214	0.8989
	5 x 5	0.8001	0.8809
	7 x 7	0.7631	0.8725

3) NOISE ADDITION ATTACK

The anticipated scheme has been assessed under noise assault on the watermarked image. The noise of different intensities has been added to the watermarked image then the watermark has been extracted from it. In Table 4, the distorted watermarked image by adding noise with different intensities to it and extracted watermark is shown. We have achieved maximum NC value on low & high noise intensity. Moreover, the achieved SSIM value of the extracted watermark is 0.9789. This shows that our scheme is performing much better. The results obtained from our experiment is shown in table 4. The results gained from the anticipated watermarking scheme described the robustness against noise attacks.

TABLE 5. Noise attack with different scaling factors.

Intensity	NC	SSIM
$\sigma = 0.001$	1	0.9789
$\sigma = 0.005$	1	0.9678
$\sigma = 0.02$	0.9712	0.8803
$\sigma = 0.01$	0.9697	0.8789

4) GEOMETRIC ATTACK

Rotation, scaling, cropping, and flipping are known as geometric image processing attacks. These geometric attacks

TABLE 6. Watermarked image and extracted watermark after Noise attack with different scaling factors.

Intensity	Watermarked Image	Extracted Watermark
$\sigma = 0.001$		
$\sigma = 0.005$		
$\sigma = 0.02$		
$\sigma = 0.01$		

TABLE 7. Different geometric attack.

Geometric Attack	NC	SSIM
Cropping	0.9223	0.8857
Rotation (20°)	0.8894	0.7071
Rotation (45°)	0.7845	0.6312
Rotation (90°)	0.5012	0.5212
Flipping	0.4561	0.6123

TABLE 8. Comparison of NC value with some existing work.

Attack Name	[48]	[49]	Proposed Work
Gaussian (0.01)	0.9727	0.968	0.9697
Median filter (3x3)	0.9570	0.969	0.9511
Average filter (3x3)	0.8945	-	0.8876
Average filter (5x5)	0.7383	-	0.7413
JPEG (Q = 40)	1	-	0.9756
JPEG (Q = 50)	1	-	0.9901

have a significant impact on the image. In Table 9, the watermarked image with different geometric attacks and the extracted watermark images have been shown. Table 5 presents the findings obtained from our experiment following the use of interpolation to geometric assaults. The effectiveness of the proposed method has significantly increased. We are considering that both the NC and SSIM values are

TABLE 9. Different geometric attack.

Geometric Attack	Watermarked Image	Extracted Watermark
Cropping		
Rotation (20°)		
Rotation (45°)		
Rotation (90°)		
Flipping		

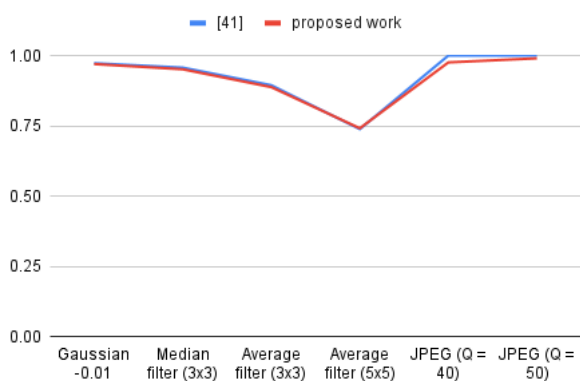


FIGURE 5. Comparison plot of NC value.

pretty high. As a result, we can say that the suggested system performs better when subjected to geometric attacks.

C. COMPARISON OF PROPOSED SCHEME WITH EXISTING SCHEMES

We have conducted a series of trials to determine how well the planned strategy actually works. The results obtained from

our experiment illustrate high NC and SSIM values. The performance can also be evaluated by comparing the results with other similar types of work. Therefore, a comparison table is shown in table 6. The maximum NC value obtained in our experiment is 0.9901 whereas the maximum NC value obtained in [48] and [45] are 1 and 0.969 respectively. The comparison has been performed between the proposed work and another similar work in [41], [45], and [48]. We can easily compare the difference between existing and proposed work from following plot shown in figure 5.

V. CONCLUSION

Using fast random transformation (FRT) and Hessenberg decomposition, a unique resilient blind image watermarking technique was developed. The concept behind this system is called “Region of Interest” (ROI). The proposed method is completely imperceptible, extremely resilient, and secure. The RONI of the cover picture is used in the recommended watermarking approach. The watermark is recovered without the cover picture being present. The suggested technique has produced watermarked photos with increased PSNR ranging from 56.9902 to 57.2356. We also attained high NC values, specifically 0.9801. The system is put through a series of tests to see how sensitive it is, and the results are contrasted with procedures. The watermark can be recovered from the image even if it has been severely distorted by JPEG compression, additive noise, median filtering, or average filtering. Better perceived quality is obtained by compressing the watermark image and extracting the watermark. NC values for the retrieved watermark’s perceptual quality range from 0.9901 to 0.9456. Experimental results show that, in terms of distortion level, our suggested solution outperforms existing state-of-the-art schemes. The suggested watermarking approach is perfect for photos with small ROI, and it delivers outstanding visual image quality in terms of PSNR, SSIM, & NC. The present work is limited only to the MRI medical images. The study is limited to only one image segmentation technique.

For future study, we suggest better method for the selection of regions, while operational trials are required prior to evaluating the watermark scheme in a fully operating PACS where medical images are preserved and retrieved. In future, more segmentation techniques will be used for separation of ROI and RONI also we will try to perform experiments on various types of DICOM images.

REFERENCES

- [1] H. Qi, D. Zheng, and J. Zhao, “Human visual system based adaptive digital image watermarking,” *Signal Process.*, vol. 88, no. 1, pp. 174–188, Jan. 2008.
- [2] J. Liu and X. He, “A review study on digital watermarking,” in *Proc. Int. Conf. Inf. Commun. Technol.*, 2005, pp. 337–341.
- [3] K. U. Singh, H. S. Abu-Hamatta, A. Kumar, A. Singhal, M. Rashid, and A. K. Bashir, “Secure watermarking scheme for color DICOM images in telemedicine applications,” *Comput., Mater. Continua*, vol. 70, no. 2, pp. 2525–2542, 2022.
- [4] A. Al-Haj and A. Amer, “Secured telemedicine using region-based watermarking with tamper localization,” *J. Digit. Imag.*, vol. 27, pp. 737–750, Jan. 2014.

- [5] E. Rayachoti, S. Tirumalasetty, and S. C. Prathipati, "SLT based watermarking system for secure telemedicine," *Cluster Comput.*, vol. 23, pp. 1223–1246, Mar. 2020.
- [6] Y. Gangadhar, V. S. G. Akula, and P. C. Reddy, "An evolutionary programming approach for securing medical images using watermarking scheme in invariant discrete wavelet transformation," *Biomed. Signal Process. Control*, vol. 43, pp. 31–40, May 2018.
- [7] T. K. Araghi and A. A. Manaf, "An enhanced hybrid image watermarking scheme for security of medical and non-medical images based on DWT and 2-D SVD," *Future Gener. Comput. Syst.*, vol. 101, pp. 1223–1246, Dec. 2019.
- [8] M. Favorskaya, E. Savchina, and K. Gusev, "Feature-based synchronization correction for multilevel watermarking of medical images," *Proc. Comput. Sci.*, vol. 159, pp. 1267–1276, Jan. 2019.
- [9] X. Liu, J. Lou, H. Fang, Y. Chen, P. Ouyang, Y. Wang, B. Zou, and L. Wang, "A novel robust reversible watermarking scheme for protecting authenticity and integrity of medical images," *IEEE Access*, vol. 7, pp. 76580–76598, 2019.
- [10] R. Mothi and M. Karthikeyan, "Protection of bio medical iris image using watermarking and cryptography with WPT," *Measurement*, vol. 136, pp. 67–73, Mar. 2019.
- [11] M. Larobina and L. Murino, "Medical image file formats," *J. Digit. Imag.*, vol. 27, no. 2, pp. 200–206, Apr. 2014.
- [12] K. U. Singh, S.-Y. Hsieh, C. Swarup, and T. Singh, "Authentication of NIFTI neuroimages using lifting wavelet transform, Arnold cat map, Z-transform, and Hessenberg decomposition," *Traitement Signal*, vol. 39, no. 1, pp. 265–274, Feb. 2022.
- [13] A. F. Qasim, F. Meziane, and R. Aspin, "Digital watermarking: Applicability for developing trust in medical imaging workflows state of the art review," *Comput. Sci. Rev.*, vol. 27, pp. 45–60, Feb. 2018.
- [14] K. U. Singh, A. Kumar, T. Singh, and M. Ram, "Image-based decision making for reliable and proper diagnosing in NIFTI format using watermarking," *Multimedia Tools Appl.*, vol. 2022, pp. 1–27, Apr. 2022.
- [15] L. O. M. Kobayashi, S. S. Furuie, and P. S. L. M. Barreto, "Providing integrity and authenticity in DICOM images: A novel approach," *IEEE Trans. Inf. Technol. Biomed.*, vol. 13, no. 4, pp. 582–589, Jul. 2009.
- [16] O. S. Pinykh, *Digital Imaging and Communications in Medicine (DICOM): A Practical Introduction and Survival Guide*, 1st ed. Cham, Switzerland: Springer, 2010.
- [17] S. A. Parah, F. Ahad, J. A. Sheikh, N. A. Loan, and G. M. Bhat, "Information hiding in medical images: A robust medical image watermarking system for E-healthcare," *Multimed Tools Appl.*, vol. 76, no. 8, pp. 10599–10633, Apr. 2017.
- [18] E. M. Abou-Nassar, A. M. Ilyyasu, P. M. El-Kafrawy, O.-Y. Song, A. K. Bashir, and A. A. El-Latif, "DITrust chain: Towards blockchain-based trust models for sustainable healthcare IoT systems," *IEEE Access*, vol. 8, pp. 111223–111238, 2020.
- [19] A. K. Singh, M. Dave, and A. Mohan, "Wavelet based image watermarking: Futuristic concepts in information security," *Proc. Nat. Acad. Sci., India, A, Phys. Sci.*, vol. 84, no. 3, pp. 345–359, Sep. 2014.
- [20] A. K. Singh, M. Dave, and A. Mohan, "Hybrid technique for robust and imperceptible multiple watermarking using medical images," *Multimedia Tools Appl.*, vol. 75, no. 14, pp. 8381–8401, 2016.
- [21] B. Gupta, D. P. Agrawal, and S. Yamaguchi, *Handbook of Research on Modern Cryptographic Solutions for Computer and Cyber Security*. Hershey, PA, USA: IGI Global, 2016.
- [22] J. M. Zain and A. R. M. Fauzi, "Medical image watermarking with tamper detection and recovery," in *Proc. Int. Conf. IEEE Eng. Med. Biol. Soc.*, Aug. 2006, pp. 3270–3273.
- [23] J. H. K. Wu, R.-F. Chang, C.-J. Chen, C.-L. Wang, T.-H. Kuo, W. K. Moon, and D.-R. Chen, "Tamper detection and recovery for medical images using near-lossless information hiding technique," *J. Digit. Imag.*, vol. 21, no. 1, pp. 59–76, Mar. 2007.
- [24] D. Boulimi, G. Coatrieux, and C. Roux, "A joint encryption/watermarking algorithm for verifying the reliability of medical images: Application to echographic images," *Comput. Methods Programs Biomed.*, vol. 106, no. 1, pp. 47–54, Apr. 2012.
- [25] L. Tan, K. Yu, A. K. Bashir, X. Cheng, F. Ming, L. Zhao, and X. Zhou, "Toward real-time and efficient cardiovascular monitoring for COVID-19 patients by 5G-enabled wearable medical devices: A deep learning approach," *Neural Comput. Appl.*, vol. 2021, pp. 1–14, Jul. 2021.
- [26] V. D. A. Kumar, S. Sharmila, A. Kumar, A. K. Bashir, M. Rashid, S. K. Gupta, and W. S. Alnumay, "A novel solution for finding postpartum haemorrhage using fuzzy neural techniques," *Neural Comput. Appl.*, vol. 2021, pp. 1–14, Jan. 2021.
- [27] S. Das and M. K. Kundu, "Hybrid contourlet-DCT based robust image watermarking technique applied to medical data management," in *Pattern Recognition and Machine Intelligence*, S. O. Kuznetsov, D. P. Mandal, M. K. Kundu, and S. K. Pal, Eds. Berlin, Germany: Springer, 2011, pp. 286–292.
- [28] M. K. Kundu and S. Das, "Lossless ROI medical image watermarking technique with enhanced security and high payload embedding," in *Proc. 20th Int. Conf. Pattern Recognit.*, Aug. 2010, pp. 1457–1460.
- [29] O. M. Al-Qershi and B. E. Khoo, "Authentication and data hiding using a hybrid ROI-based watermarking scheme for DICOM images," *J. Digit. Imag.*, vol. 24, no. 1, pp. 114–125, Nov. 2009.
- [30] S. Rastegar, F. Namazi, K. Yaghmaie, and A. Aliabadian, "Hybrid watermarking algorithm based on singular value decomposition and radon transform," *AEU-Int. J. Electron. Commun.*, vol. 65, no. 7, pp. 658–663, Jul. 2011.
- [31] F. Cao, H. K. Huang, and X. Q. Zhou, "Medical image security in a HIPAA mandated PACS environment," *Computerized Med. Imag. Graph.*, vol. 27, nos. 2–3, pp. 185–196, Mar. 2003.
- [32] E. D. Tsougenis, G. A. Papakostas, D. E. Koulouriotis, and V. D. Tourassis, "Performance evaluation of moment-based watermarking methods: A review," *J. Syst. Softw.*, vol. 85, no. 8, pp. 1864–1884, Aug. 2012.
- [33] C. K. Tan, J. C. Ng, X. Xu, C. L. Poh, Y. L. Guan, and K. Sheah, "Security protection of DICOM medical images using dual-layer reversible watermarking with tamper detection capability," *J. Digit. Imag.*, vol. 24, no. 3, pp. 528–540, Jun. 2011.
- [34] M. N. Ahmed, S. M. Yamany, N. Mohamed, A. Farag, and T. Moriarty, "A modified fuzzy C-means algorithm for bias field estimation and segmentation of MRI data," *IEEE Trans. Med. Imag.*, vol. 21, no. 3, pp. 193–199, Mar. 2002.
- [35] A. M. Bensaid, L. O. Hall, J. C. Bezdek, and L. P. Clarke, "Partially supervised clustering for image segmentation," *Pattern Recognit.*, vol. 29, no. 5, pp. 859–871, May 1996.
- [36] A. G. Radwan, S. H. AbdElHaleem, and S. K. Abd-El-Hafiz, "Symmetric encryption algorithms using chaotic and non-chaotic generators: A review," *J. Adv. Res.*, vol. 7, no. 2, pp. 193–208, 2016.
- [37] R. Eswaraiiah and E. S. Reddy, "Medical image watermarking technique for accurate tamper detection in ROI and exact recovery of ROI," *Int. J. Telem. Appl.*, vol. 2014, pp. 1–10, Jan. 2014.
- [38] H.-T. Wu, J. Huang, and Y.-Q. Shi, "A reversible data hiding method with contrast enhancement for medical images," *J. Vis. Commun. Image Represent.*, vol. 31, pp. 146–153, Aug. 2015.
- [39] K. Balasamy and S. Ramakrishnan, "An intelligent reversible watermarking system for authenticating medical images using wavelet and PSO," *Cluster Comput.*, vol. 22, no. S2, pp. 4431–4442, Mar. 2019.
- [40] R. Rhouma, E. Solak, and S. Belghith, "Cryptanalysis of a new substitution-diffusion based image cipher," *Commun. Nonlinear Sci. Numer. Simul.*, vol. 15, no. 7, pp. 1887–1892, 2010.
- [41] L. Kumar and K. U. Singh, "Color ultrasound image watermarking scheme using FRT and Hessenberg decomposition for telemedicine applications," *JUCS-J. Universal Comput. Sci.*, vol. 28, no. 9, pp. 882–897, Sep. 2022.
- [42] S. AlZubi, N. Islam, and M. Abbod, "Multiresolution analysis using wavelet, ridgelet, and curvelet transforms for medical image segmentation," *Int. J. Biomed. Imag.*, vol. 2011, Sep. 2011, Art. no. 136034.
- [43] C. Mira, D. Fournier-Prunaret, L. Gardini, H. Kawakami, and J. C. Cathala, "Basin bifurcations of two-dimensional noninvertible maps: Fractalization of basins," *Int. J. Bifurcation Chaos*, vol. 4, no. 2, pp. 343–381, Apr. 1994.
- [44] G. Golub, S. Nash, and C. Van Loan, "A Hessenberg-Schur method for the problem $AX + XB = C$," *IEEE Trans. Autom. Control*, vol. AC-24, no. 6, pp. 909–913, Dec. 1979.
- [45] M. C. J. Christ and R. M. S. Parvathi, "Fuzzy c-means algorithm for medical image segmentation," in *Proc. 3rd Int. Conf. Electron. Comput. Technol.*, Apr. 2011, pp. 33–36.
- [46] *Fair Benchmark for Image Watermarking Systems*, SPIE, Bellingham, WA, USA, 1999.
- [47] Z. Wang, A. C. Bovik, and H. R. Sheikh, "Structural similarity based image quality assessment," in *Digital Video Image Quality and Perceptual Coding*. Boca Raton, FL, USA: CRC Press, 2017, pp. 225–242.

- [48] V. S. Verma, R. K. Jha, and A. Ojha, "Significant region based robust watermarking scheme in lifting wavelet transform domain," *Expert Syst. Appl.*, vol. 42, no. 21, pp. 8184–8197, Nov. 2015.
- [49] X. Zhang, W. Zhang, W. Sun, T. Xu, and S. Kumar Jha, "A robust watermarking scheme based on ROI and IWT for remote consultation of COVID-19," *Comput., Mater. Continua*, vol. 64, no. 3, pp. 1435–1452, 2020.



KAMRED UDHAM SINGH received the Ph.D. degree from Banaras Hindu University, India, in 2019. From 2015 to 2016, he was a Junior Research Fellow and from 2017 to 2019, he was a Senior Research Fellow at University Grant Commission (UGC), India. In 2019, he became an Assistant Professor at the School of Computing, Graphic Era Hill University, India. He is currently a Postdoctoral Fellow with the Department of Computer Science and Information Engineering, National Cheng Kung University, Taiwan. He has published several research articles in international peer-reviewed journals. His research interests include image security and authentication, deep learning, medical image watermarking, and steganography.



LALAN KUMAR (Graduate Student Member, IEEE) is currently pursuing the Ph.D. degree in digital watermarking with Graphic Era Hill University, Dehradun, India. He has been working as an Assistant Professor with the Department of Master of Computer Applications, G. L. Bajaj Institute of Technology and Management, Greater Noida, since 2015. He has a teaching experience of more than 14 years with reputed institutions of India. He has several research articles in journals of national and international repute. His research interests include AI/ML, cryptography, and social media.



SURBHI BHATIA received the Ph.D. degree in computer science and engineering in the area of machine learning and social media analytics from Banasthali University, in 2018. She is currently working with the Department of Information Systems, College of Computer Sciences and Information Technology, King Faisal University, Saudi Arabia. She has more than ten years of academic and teaching experience in different universities in India and Saudi Arabia. She has published ten international patents from India, Australia, and USA. She has published many papers in reputed journals and conferences in high indexing databases (SCI, SCIE, Scopus, Web of Science, ESCI). She has delivered talks as a keynote speaker in IEEE conferences and in faculty development programs. She has conducted workshops for AICTE programmers and chaired technical sessions in many conferences. She has successfully authored two books from Springer and Wiley. She has also edited ten books from CRC Press, Elsevier, and Springer. She has completed ten projects approved by Ministry of Education, Saudi Arabia, and Deanship of Scientific Research in different universities, Saudi Arabia and India. Her research interests include knowledge management, information systems, artificial intelligence, and data analytics. She has been awarded as the Research Excellence Award from King Faisal University. She received the Project Management Professional Certification from reputed Project Management Institute, USA. She is the Chair of the Research Committee with the Information Systems Department. She is also serving as a Guest Editor for Special Issues in reputed journals of Springer (*SN Applied Sciences*, Indexing ESCI, Springer), *Computer, Materials and Continua* (Indexing SCI, Scopus), *Internet of Things* (Indexing SCIE, Elsevier), Hindawi, Bentham Science, an Academic Editor of *Computational Intelligence and Neuroscience* and *PLOS ONE* journal, and an Associate Editor of *HCIS*.



ANKIT KUMAR is currently working as an Assistant Professor with the Department of Computer Engineering and Applications. He has published multiple papers in Taylor and Francis's different journals related to networks. His articles are published in 54 international journals and 11 national journals. He has received eight patents. His work has been profiled broadly, such as in information security, cloud computing image processing, neural networks, and networks. His research interests include wireless sensor networks, computer networks, information security, computational model, compiler design, and data structure. He is a reviewer and editor of many reputed journals.

ALHANOF KHALID ALMUTAIRI received the B.Sc. degree in information science from the University of Otago, New Zealand, in 2012, the M.Sc. degree (Hons.) in information technology from the University of Nottingham, U.K., in 2015, and the Ph.D. degree in computer science from The University of Auckland, New Zealand, in 2022. She is currently working as a Lecturer with the College of Computer Science and Information Technology, King Faisal University. Her research interests include information systems, software development, business process management, and IT governance. She has served as a reviewer for multiple conferences.



MOHD ASIF SHAH is currently working as an Associate Professor at Kebri Dehar University, Ethiopia. He has more than fifty publications which are indexed in Scopus, and Web of Science Indexed Journals. Having more than ten years of teaching experience, he has been a popular instructor.

His courses always fill up quickly as students enjoy his teaching style. He tries to deliver the information in a fun and interesting manner to aid students' grasp of the material and hold their interest.

...